Atmos. Chem. Phys. Discuss., doi:10.5194/acp-2017-43, 2017
Manuscript under review for journal Atmos. Chem. Phys.
Discussion started: 10 February 2017

Atmospheric Chemistry and Physics Discussions

Net ecosystem exchange and energy fluxes in a West Siberian bog

Pavel Alekseychik[1], Ivan Mammarella[1], Dmitri Karpov[2], Sigrid Dengel[6], Irina Terentieva[3], Alexander Sabrekov[2,3], Mikhail Glagolev[2,3,4,5] and Elena Lapshina[2]

[1]Department of Physics, P.O. Box 68, FI-00014, University of Helsinki, Finland
[2]Department of Environmental dynamics and global climate change, 628012, Yugra State University, Russia
[3]Tomsk State University, Russia
[4]Department of Soil Physics and Development, 119991, Moscow State University, Russia
[5]Institute of Forest Science, Russian Academy of Sciences, 143030, Moscow, Russia
[6]Climate and Ecosystem Sciences Division, Lawrence Berkeley National Laboratory, Berkeley, USA

Correspondence to: Pavel Alekseychik (pavel.alekseychik@helsinki.fi)

Abstract. Very few studies of ecosystem-atmosphere exchange involving eddy-covariance data have been conducted in Siberia, with none in West Siberian middle taiga. This work provides the first estimates of carbon dioxide (CO_2) and energy budgets at a typical bog of the West Siberian middle taiga based on May-August measurements in 2015. The footprint of measured fluxes consisted of homogeneous mixture of tree-covered ridges and hollows with the vegetation represented by typical sedges and shrubs. Generally, the surface exchange rates resembled those of pine-covered bogs elsewhere. The surface energy balance closure was 90%. Net CO_2 uptake was comparatively high, summing up to 196 gC m^{-2} for the four measurement months, while the Bowen ratio was typical at 30%. The ecosystem turned into a net CO_2 source during several front passage events in June and July. Several periods of heavy rain helped keep the water table at a constant level, preventing a usual drawdown in summer. However, because of the cloudy and rainy weather, the observed fluxes might rather represent the special weather conditions of 2015 than their typical level.

1. Introduction

Boreal peatlands, covering a large fraction of the northern hemisphere, are an important terrestrial carbon pool, whose size is estimated to be around 500 ± 100 Pg of organic carbon integrated over the entire peat depth (Yu, 2012). Photosynthesis and respiration of plant and microbial communities regulate the size of this pool. However, peatlands are also prone to rapid ecological changes related to climate, which modify the interaction between hydrology, carbon cycle, vegetation cover and micro-topography. Detailed knowledge of the processes governing the carbon exchange in northern peatlands over the course of a growing season is limited, especially with respect to the impact of relevant environmental variables.

While continuous and long-term time series of carbon dioxide (CO_2), sensible and latent heat fluxes are already available from several boreal peatland sites in Europe, measurements of this kind are rare in Siberia. This is mainly due

to the lack of developed measurement sites with the infrastructure suitable for continuous monitoring of the ecosystem-atmosphere exchange processes, and frequent inaccessibility of key ecological zones and biomes. In remote and large areas such as West Siberia, current estimates of greenhouse gas emission rates are largely uncertain, because discontinuous and short-term observations (static chamber technique) have often been used to derive regional and long term emission rates (Golovatskaya and Dyukarev, 2008;Schneider et al., 2011;Glagolev et al., 2011;Sabrekov et al., 2013). Currently, only about ten eddy-covariance (EC) flux tower sites are active in Russia east of the Urals (Alekseychik et al., 2016). Previous studies using this method in Boreal peatlands have shown the importance of temperature, solar radiation, and water table depth in controlling the net ecosystem exchange (NEE) (Arneth et al., 2002;Aurela, 2004;Lafleur et al., 2003;Friborg et al., 2003;Humphreys et al., 2006). Most studies show that, during the growing season, peatlands are net sinks for CO_2. However, during warm and dry growing seasons the peatland sink strength is notably reduced and in some cases lead to net CO_2 losses (Bubier et al., 2003;Lafleur et al., 2003).

In order to fill the West Siberian measurement gap, we have recently established a new EC flux tower at the raised bog site at the Mukhrino field station in Khanty–Mansi Autonomous Okrug (Russia). The Mukhrino field station is officially part of the PEEX station network (Alekseychik et al., 2016) and INTERACT (http://www.eu-interact.org/). The energy and carbon dioxide flux data provided by the eddy-covariance tower is so far unique for West Siberian middle taiga and is the only setup functioning as of 2016 in West Siberia (within at least a radius of 1000 km). The aims of this study are to present and analyze the new flux data tower with the related ancillary measurements, to investigate the diurnal and seasonal variations of NEE and energy fluxes, as well as to determine summertime budgets of energy and CO_2 of the ecosystem.

2. Materials

2.1 Site description

The Mukhrino Field Station (60°54' N, 68°42' E) is located at the east terrace of the Irtysh River 20 km south of the point of confluence with the Ob' river in the middle taiga zone of the West Siberian Lowland (WSL). WSL is a geographical region of Russia bordered by the Ural Mountains in the west and the Yenisey River in the east; the region covers 2.75×10^6 km^2 from 62-89˚ E to 53-73˚ N. Paludification in WSL started after a climate warming 11500 cal. BP with 55% of the present C store accumulated by 6 000 cal. BP; the mires have expanded very little during the past 3000 years (Turunen et al., 2001). Middle taiga (59-62˚ N) covers about 56.6 Mha in the central part of the WSL; the region features flat terrain with elevations of 80 to 100 m above sea level.

The region has a subarctic or boreal climate (Köppen-Geiger code Dfc) with a long cold winter, a short warm summer and frequent change of weather conditions. Average monthly air temperatures range from -20 to 18 °C over the year with the mean annual temperature of -1.1 °C. The latter increased by 0.4 °C from 1893-1935 to 1970-1999 period (Bulatov, 2007). Median annual precipitation is 520 mm, and evapotranspiration is 445 mm (Bulatov, 2007). Mean summer precipitation is 208 mm, ranging from 74 mm to 354 mm over the period from 1934 to 2014. Continuous permafrost is absent. Peat soils freeze to a depth of about 50 cm. Typically, snowmelt and river break up start in the first half of May. Mean duration of snow cover period is 180 days (from 19 October to 25 April) with the average March snow depth 54 cm. Growing season lasts for 98 days (Bulatov, 2007); the number of growing degree-days >5 °C is from 900 to 1500 (median – 1250).

The excess water supply and flat terrain with poor drainage provides favorable conditions for wetland formation in the region. Large wetland systems commonly cover watersheds (34% of the zonal area) and have a convex dome with

Atmos. Chem. Phys. Discuss., doi:10.5194/acp-2017-43, 2017
Manuscript under review for journal Atmos. Chem. Phys.
Discussion started: 10 February 2017

Atmospheric Chemistry and Physics Discussions

centers that are 3 to 6 m higher than the periphery. The wetland subtypes here have strict spatial regularities. Ridge-hollow-lake complexes (15% of the total wetland area) represent central plateau depressions with stagnant water. They consist of numerous small lakes up to 2 m deep with peat bottom and waterlogged hollows. Different types of ridge-hollow complexes dominate (42%), covering the better drained gentle slopes. Pine bogs (28%) are more frequent in drier areas, where the peat surface is typically 10-50 cm above the water table level. Poor and rich fens (8%) develop along the wetland edges and watercourses, where the nutrient availability is higher. Open bogs with mosaic dwarf shrubs-sphagnum vegetation are widespread (5%) at the periphery of individual wetland bodies. Wooded swamps (2%) surround the peatland systems (Terentieva et al., 2015). Primary lakes of 100-2000 m in diameter and up to 5 meters depth with mineral bottom are widespread.

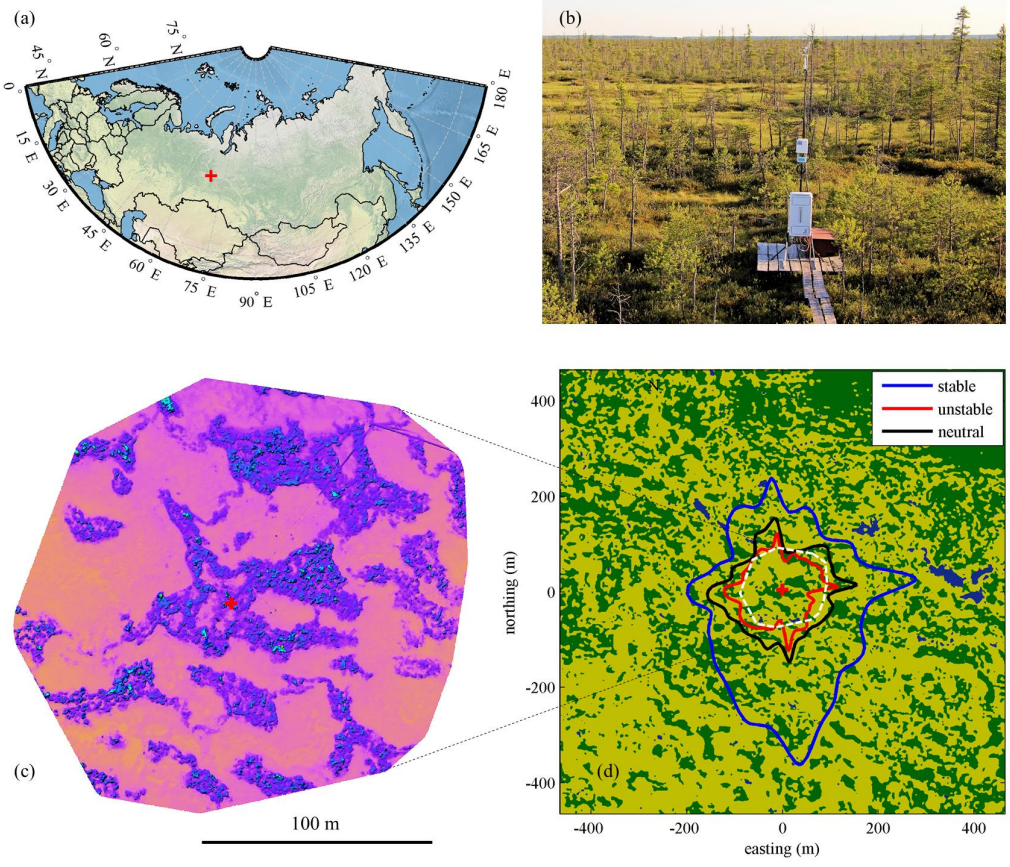

Figure 1: (a) map showing the Mukhrino station location, (b) photo of the EC tower facing southwest, (c) digital elevation map based on drone survey, (d) surface type classification map. (d) includes an eddy-covariance footprint overlay, with the isolines delineating the 70% cumulative EC source zone in the three stability classes. Color coding in (d): dark green – ridges/hummocks, light green – lawns/hollows, dark blue – ponds. The red cross marks the location of the EC tower.

The Mukhrino Field Station (map, Fig. 1a) is located on the eastern edge of a peatland 10 km × 5 km size. The study site is considered to be representative of raised bogs, a peatland type dominant not only in the west (Masing et al., 2010) but also in the other parts of Siberia (Shulze et al., 2015). It has a peat layer of up to 5 meters in depth that is composed of Sphagnum peat with minor contributions by other plants. Mean pH is from 3.5 to 5, electric conductivity – from 0 to 200 μSm/m^2 (Sabrekov et al., 2011). The rate of peat accumulation at the nearby wetland was 0.35 mm yr^{-1}, while the average dry bulk density of the peat was 92.7 g dm^{-3} with the average C peat content of 52.7% (Turunen et al., 2001).

Pine bogs and ridge-hollow complexes are dominant within the boundaries of Mukhrino bog (Fig. 1b-d). The tree cover of ridges and pine bogs is represented by stunted *Pinus sylvestris*. Their dwarf shrub layer consists of *Ledum palustre*, *Andromeda polifolia*, *Chamaedaphne calcylata*, *Vaccinium vitis-idaea*, *Vaccínium uliginosum*, *Oxycoccus palustris.* Herbs are represented by *Rubus chamaemorus* and a few tiny species of sundews (*Drosera anglica*, *D. intermedia*, *D. rotundifolia*). *Carex limosa*, *Eriophorum vaginatum*, *Scheuchzeria palustris* are widespread within oligotrophic hollows of ridge-hollow complexes. The moss layer of raised bogs consists of Sphagnum mosses as *S. fuscum*, *S. lindbergii*, *S. balticum*, *S. papillosum*, *S. angustifolium*, *S. magellanicum*, *S. jensenii*, etc. The area fractions of open water, hollows and ridges within a 200m radius around the flux tower are 1%, 67% and 32%, correspondingly (Fig. 1c-d).

Over the past years the Mukhrino bog has been the focus of a large number of studies ranging from surface-atmosphere gas exchange (Glagolev et al., 2011) to geochemistry and physical, chemical and biochemical properties of peat(Stepanova and Pokrovsky, 2011;Szajdak et al., 2016), hydrology (Bleuten and Filippov, 2008), microbiology including mycology (Filippova et al., 2015).

2.2 Measurements

Turbulent fluxes of momentum, sensible (H) and latent (LE) heat, and CO_2 were measured between May and September 2015 with the eddy-covariance (EC) technique. The EC system included a 3-D ultrasonic anemometer (Gill R3, Gill Instruments Limited, Great Britain) providing three wind velocity components and the sonic temperature, and an open-path infrared gas analyzer (LI-7500, LI-COR Biosciences, USA) for the measurement of CO_2 and water vapor (H_2O). The EC sensors were mounted on a tower at a 4 m height above the peat surface. The horizontal separation between the sonic anemometer and the gas analyzer was 15 cm. The open-path gas analyzer was connected to the analogue input of the sonic anemometer. Data were logged via serial cable using a mini-computer with a sampling frequency of 10 Hz.

Auxiliary parameters were measured and recorded by two automatic meteorological stations located within 30 m from the EC tower. The measured parameters include the soil temperature profile at depths of 2, 5, 10, 20 and 50 cm (thermocouple sensors), net radiation (Kipp&Zonen NRLite radiometer), incoming and reflected photosynthetically active radiation (Li-Cor LI-190SA Quantum Sensor), air temperature and relative humidity (ROTRONIC HygroClip S3) and precipitation (HOBO Data Logging Rain Gauge RG3-M). Water table level was measured in two locations (hollow and ridge) by Mini-Diver water level sensors (DI 501).

The station uses an autonomous power supply system consisting of solar panels (4 kW in total) and a wind vane generator (3 kW). A combined charge controller/invertor unit charges the batteries with the total capacity of 800 Ah and supplies up to 3 kW to the field station. In wintertime, a 2.5 kW petrol generator is additionally used.

3. Methods

3.1 Flux calculation

Atmos. Chem. Phys. Discuss., doi:10.5194/acp-2017-43, 2017
Manuscript under review for journal Atmos. Chem. Phys.
Discussion started: 10 February 2017

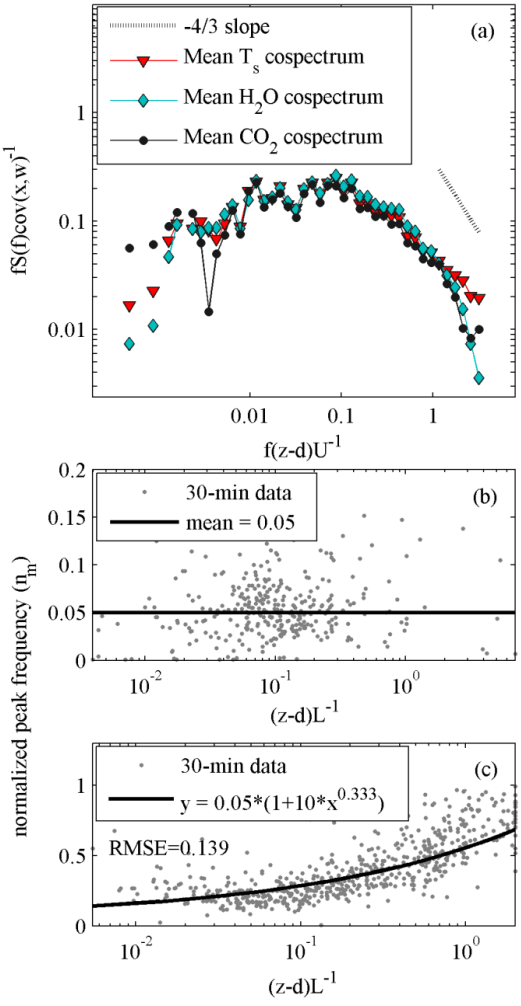

Figure 2: (a) Normalized frequency-weighted co-spectra of temperature, carbon dioxide and water vapour as a function of normalized frequency measured on 16 July 2015, 11:00-13:30 (mean value of stability parameter $(z-d)L^{-1}$ = -0.023). The two following subplots show the 30 min values of the normalized peak frequency n_m *versus* the stability parameter (z-d)/L in unstable condition (b) and stable conditions (c).

The post-field processing of EC rawdata was performed with EddyUH software (Mammarella et al., 2016). Fluxes of sensible and latent heat and CO_2 were calculated as the 30-min block- averaged covariances between the scalars and the vertical wind velocity:

$$H = \rho_d c_p \overline{w'T_a'} \quad (1)$$

$$LE = \rho_d L_v \frac{M_w}{M_a} \overline{w'\chi_{H_2O}'} \quad (2)$$

$$F_{co_2} = \frac{\rho_d}{M_a} \overline{w'\chi_{CO_2}'} \quad (3)$$

where ρ_d is the dry air density (kg m^{-3}), c_p the specific heat capacity of dry air (J kg^{-1} K^{-1}), L_v is the latent heat of vaporization for water (J kg^{-1}), T_a the air temperature (K) and M_a and M_w the molar masses of dry air and water, respectively. The terms $\overline{w'T_a'}$, $\overline{w'\chi_{H_2O}'}$ and $\overline{w'\chi_{CO_2}'}$ are the covariances between w and T_a, dry mole fractions of CO_2 and H_2O, respectively.

Data were de-spiked according to standard methods (Vickers and Mahrt, 1997), thereafter wind velocity components were rotated into a natural coordinate system by performing a two-step rotation to each 30 min interval setting the x axis along the mean wind direction and zeroing the mean vertical wind velocity. The time delay between the vertical wind speed w and the scalar (CO_2 or H_2O) was derived for each 30 min interval by maximizing the respective cross-correlation function, calculated in a very narrow window (from -0.5 s to 0.5 s). The fluxes were corrected for high and low frequency losses that occur due to the limited frequency response of the EC system and the finite time averaging period used for calculating the fluxes, respectively. Correction was done according to Mammarella et al. (2009) by using experimentally and theoretically determined co-spectral transfer functions at high and low frequency. The estimated low pass filter time constant for CO_2 and H_2O was 0.05 s. The effect of this correction is very small, and is mainly caused by the separation between the open-path analyzer and the sonic anemometer. The high frequency attenuation can be clearly seen in the measured co-spectra (Fig. 2a). When performing the spectral correction to the CO_2 and H_2O fluxes, the derived transfer functions were used together with the site-specific co-spectral model, which was estimated by a non-linear fit of the measured $\overline{w'T'}$ co-spectrum. The normalized frequency of the co-spectral peak (n_m) was also estimated from the co-spectrum for each 30 min record, and the site-specific stability dependence was established (Fig. 2b-c). In unstable conditions (stability parameter z/L<0) n_m has a constant value of 0.05, whereas in stable conditions an increase with atmospheric stability is observed (z/L>0). Before calculating the sensible heat flux, the 30 min sonic temperature covariances are converted to actual air temperature covariances following the approach of van Dijk et al. (2004). Finally, LE and CO_2 fluxes are corrected for air density fluctuations (Webb et al., 1980).

Ground heat flux (G) was calculated from the peat temperature profile as heat storage change in the top 50 cm of soil following the methodology described in Ochsener et al. (2007) and elsewhere:

$$G = \int_0^{50cm} C_v \frac{\partial T}{\partial t} dz \quad (4)$$

The total volumetric heat capacity, C_v, was calculated as a sum of volumetric heat capacities of the solid, water and air constituents, weighted by their volume fractions in the soil matrix. Volumetric soil water content profile was modeled as a function of water level (Yurova et al., 2007;Weiss et al., 1998):

$$\theta(z) = \phi[1+(a(-(WT-z)))^b]^{-1+1/b} \quad (5)$$

where ϕ is the soil porosity and a, b the empirical parameters. ϕ was taken as 95%, corresponding to the average of the representative acrotelm and catotelm values (Granberg et al., 1999). Therefore, the fraction of solid peat particles constituted the remaining 5% of the volume. a and b were adopted from Yurova et al. (2007).

Atmos. Chem. Phys. Discuss., doi:10.5194/acp-2017-43, 2017
Manuscript under review for journal Atmos. Chem. Phys.
Discussion started: 10 February 2017

Atmospheric Chemistry and Physics Discussions

3.2 Flux quality criteria and footprint

In this study, we analyzed the EC data from the period 1st of May to 31st of August 2015 (122 days). A long gap in CO_2 and H_2O flux data, due to IRGA malfunction, occurred between 25 July and 6 August 2015. Short gaps during night time amount to 77% of the total night time periods, being mainly due to limited power availability, but also low turbulence conditions. Other instrumental problems causing spikes in the measured CO_2 and H_2O signals (mainly caused by rain) were eliminated by the despiking method as described in Sect. 3.1 and by visual inspection of the raw data timeseries. The 30 min time series containing more than 5 spikes were discarded from further analysis, causing a loss of about 4% of CO_2 and H_2O data and 13% of sonic anemometer data. Only the 30 min records with friction velocity (u_*) larger than 0.1 m/s were used in further analyses. Finally, the overall data coverage for quality-controlled and filtered CO_2, sensible and latent heat fluxes during the selected period was 35%, 38% and 36%, respectively. CO_2 nocturnal data of August was affected by spikes and so excluded from analysis.

Flux footprint was estimated using the Kormann and Meixner (2001) model. In the calculations, a value of 0.12 m (an average for May-August calculated from sonic anemometer data assuming a logarithm wind profile in near-neutral stability conditions) for the aerodynamic roughness length was used, whereas wind speed, Obukhov length and standard deviation of lateral wind velocity component were acquired from the EC data. The average source area contributing to 70% of the flux ranges from 89 m in unstable conditions up to about 116 m in near-neutral and 202 m in stable conditions (Fig. 1d).

3.3 Partitioning of Net Ecosystem Exchange

The net ecosystem exchange (NEE) measured by EC was partitioned into ecosystem gross primary production (GPP) and ecosystem respiration (R_e). The R_e model (R_{mod}) was calculated from a Q10-type temperature response curve fitted to the night-time EC data, when respiration is the only component of NEE. Night-time was defined as all the periods when the solar elevation angle was lower than 5°. Peat temperature at a 5 cm depth was used as the driver of R_e, and the following equation

$$\mathrm{R}_{\mathrm{mod}} = R_{ref} Q_{10}^{\left(\frac{T_0 - T_{ref}}{10}\right)} \quad (6)$$

was fitted to the NEE data (Fig. 3a), where T_0 is the peat temperature at a 5 cm depth (˚C), T_{ref} the reference temperature of 12˚C, R_{ref} the reference respiration of 0.8 μmol(CO_2) m^{-2} s^{-1}, and Q_{10} the temperature sensitivity of 2.3.

Then, a gross primary productivity (GPP) estimate was calculated by subtracting R_e from the EC-derived NEE. In order to gap-fill the GPP time series, a Michaelis-Menthen-type model employing photosynthetically active radiation (PAR) as a driver was used,

$$GPP_{\mathrm{mod}} = \frac{P_{\max} PAR}{k + PAR} \quad (7)$$

The fitting procedure was executed within a 30-day moving time window (Fig. 3b). The GPP model parameter values so obtained were then smoothed out with the spline interpolation procedure and rescaled down to the 30-minute resolution of the original data. Finally, the model GPP for 30-min average values of P_{max}, k and PAR was calculated from Eq. (7).

Atmos. Chem. Phys. Discuss., doi:10.5194/acp-2017-43, 2017
Manuscript under review for journal Atmos. Chem. Phys.
Discussion started: 10 February 2017

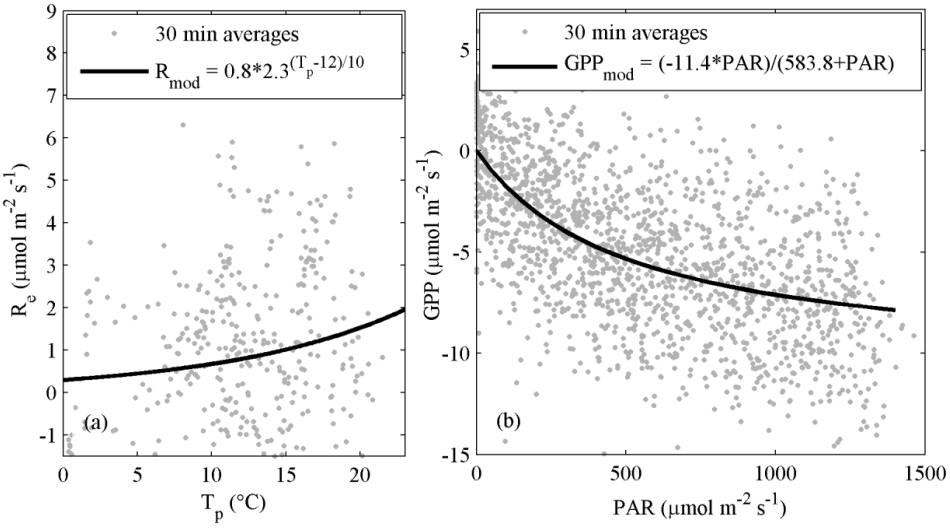

Figure 3: (a) Night-time ecosystem respiration as a function of peat temperature at 5 cm depth; (b) average light response function fit to all available data.

4. Results and discussion

4.1 Environmental conditions

Air temperature fluctuations during the summer season of 2015 at Mukhrino were unusual for the local climate. The spring was early and warm: the average air temperatures in May and June were 4.1 °C, or 3.4 °C higher than the long-term average (Fig. 4a). It caused dramatic snowmelt with a further increase of peatland water table level in May-June. The beginning of June was characterized by a lowered air temperature; average July and August values sunk below the average by 2.7 and 1.7°C, respectively. In contrast to most previous years, June was the warmest month with an average air temperature of 18˚C and a maximum value of 32˚C. Maximum soil temperature at a 20 cm depth (21 °C) was observed in the last decade of June, while soil temperature at 50 cm had two maxima of 16°C in beginning of July and in first decade of the August (Fig. 4a). Photosynthetically active radiation was at its maximum in May-June, slightly decreasing in July and August (Fig. 4b). The maximum midday value of 1463 μmol m^{-2} s^{-1} was registered in the middle of June.

Atmos. Chem. Phys. Discuss., doi:10.5194/acp-2017-43, 2017
Manuscript under review for journal Atmos. Chem. Phys.
Discussion started: 10 February 2017

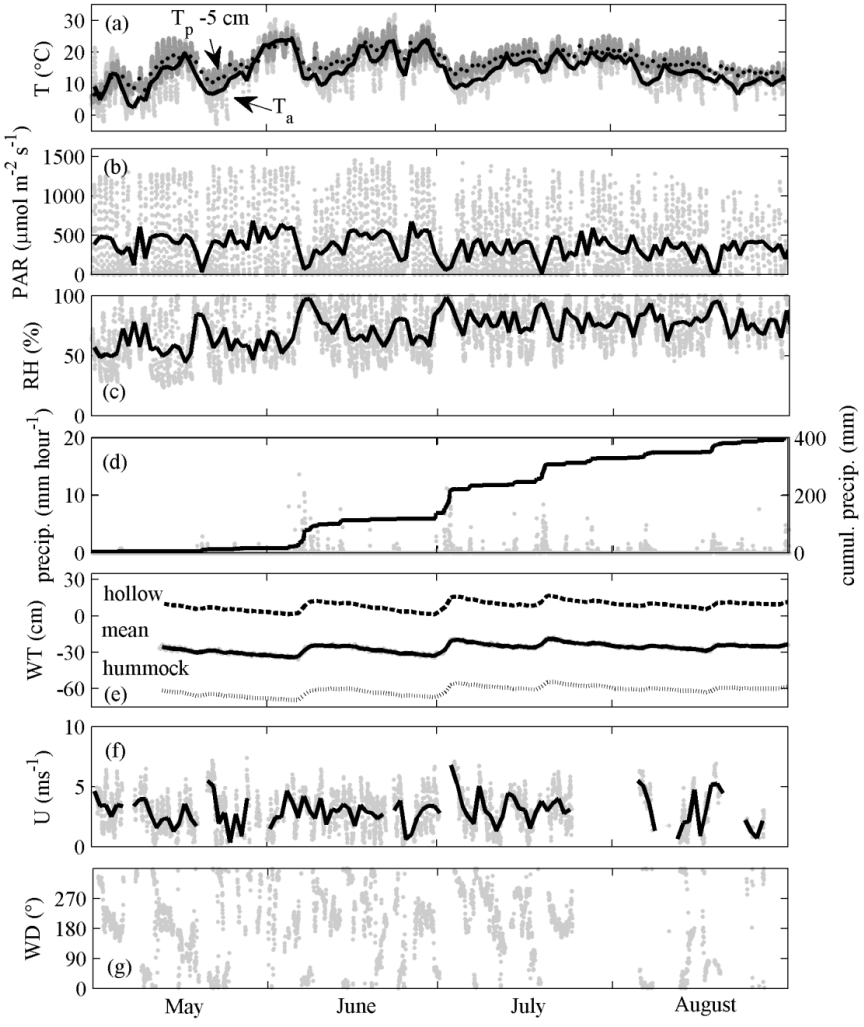

240 **Figure 4:** Time series of the environmental variables. The grey dots are 30 min measurements, while the black lines represent daily averages, except in (d) where a bold line shows the cumulative precipitation.

Precipitation considerably differed from the 81-year reference period (not shown). It was 2.7 times higher in June-July because of three heavy rainfall periods (4-9 June, 2-5 July, 18-20 July 2015). The total cumulative precipitation of the
245 study period (May-August) was 405 mm or 45% higher comparing to the reference period, and 325 mm in May-July (Fig. 4d). Accordingly, the water table depth (WTD) changes follow the intensity and frequency of precipitation, decreasing slowly during dry periods, and rapidly increasing in heavy rain (Fig. 4e). The snow resided on the ground until 28 April and after 30 September in 2015.

The prevailing wind direction was from the South/South-West (150-260˚, 45% of cases), in which the proportions of
250 open water, hollows and ridges within the 200 m radius are 1%, 67% and 32%, correspondingly. The same proportions hold for the entire area within the 200 m radius around the mast, implying high anisotropy of surface types.

Atmos. Chem. Phys. Discuss., doi:10.5194/acp-2017-43, 2017
Manuscript under review for journal Atmos. Chem. Phys.
Discussion started: 10 February 2017

Atmospheric Chemistry and Physics Discussions

4.2 Surface energy exchange

Time series of the surface energy fluxes and their monthly diurnal course are shown in Figs. 5-6. The midday net radiation (R_n) averaged 400 W m^{-2} and 380 W m^{-2} in May and June, respectively, because of the large amount of incoming solar radiation (Fig. 4). Moreover, the high water level after snowmelt resulted in low albedo and relative high R_n. On the other hand, the midday values in the second part of the summer are clearly lower, being 300 W m^{-2} and 280 W m^{-2} in July and August, respectively. In fact, later on during the summer the water level decreases, the ground vegetation probably has a higher reflectivity increasing the surface albedo and decreasing R_n. In addition, because of slightly larger number of overcast days (16 in July and 17 in August), the amount of incoming solar radiation is lower as compared with May and July (Table 1). Heat is stored in the soil throughout the studied period, but the average flux is very small, ranging from 7.6 W m^{-2} in May to 0.7 W m^{-2} in August. Most of the available energy is released as latent heat, whose monthly averaged fluxes are between 59.8 and 100.3 W m^{-2}, while sensible heat fluxes are more than three times lower ranging from 30.3 W m^{-2} in July to 16.4 W m^{-2} in August (Table 1).

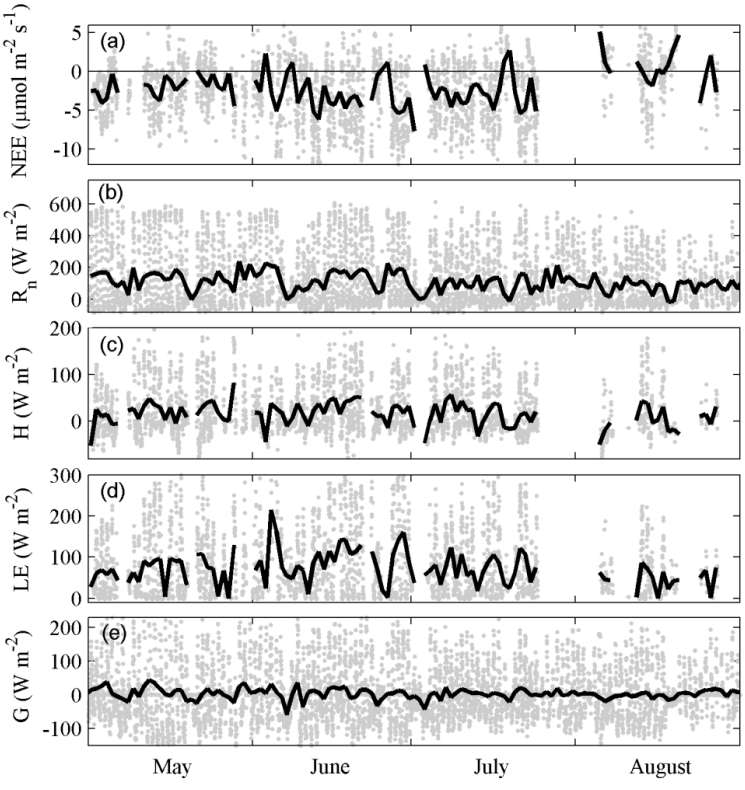

Figure 5: Time series of the surface fluxes measured with the eddy-covariance system. The grey dots are 30 min measurements, while the black line represents daily averages.

Atmos. Chem. Phys. Discuss., doi:10.5194/acp-2017-43, 2017
Manuscript under review for journal Atmos. Chem. Phys.
Discussion started: 10 February 2017

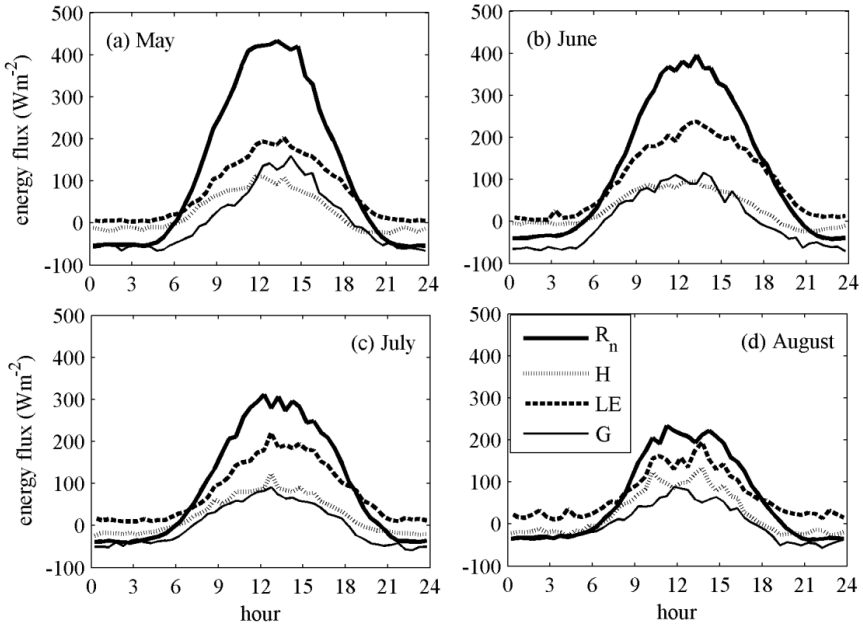

Figure 6: Monthly average diurnal courses of the energy balance components. The time shown in the x-axis is local winter time (UTC+5).

There is a clear seasonal change in LE, which starts to increase rapidly in May due to high R_n values, reaching the daily mean peak in July (239 W m^{-2}), and then decreases in July reaching the minimum value of about 140 W m^{-2} in August (Fig. 5 and Table 1).

Table 1. Monthly averages of air temperature (T_a), soil temperature at 5 cm depth (T_p), photosynthetic active radiation (PAR), cumulative precipitation (mm), net radiation (R_n), ground heat flux (G), sensible heat flux (H), latent heat flux (LE), Bowen ratio (ß), energy balance residual (Res = R_n-H-LE-G), and energy balance closure (EBC = (H+LE+G)/(R_n)).

	T_a [°C]	T_p [°C]	PAR [Wm^{-2}]	P [mm]	WTD [cm]	R_n [Wm^{-2}]	G [Wm^{-2}]	H [Wm^{-2}]	LE [Wm^{-2}]	ß [-]	Res [Wm^{-2}]	EBC [%]	NEE [gC m^{-2}]
May	11.1	10.1	399.0	12.2	-28.6	129.6	7.6	23.2	74.5	0.31	18.8	87	-35
June	18.0	18.1	403.9	121.2	-28.5	128.6	3.3	30.3	100.3	0.30	-7.1	105	-68
July	15.0	16.9	321.1	191.4	-22.7	92.6	1.3	22.7	75.5	0.30	-2.2	102	-77
August	12.6	13.4	247.1	80.0	-26.7	75.9	0.7	16.4	59.8	0.27	-20.6	129	-15
May-August	14.3	14.6	342.3	404.8	-26.4	107.7	3.2	24.7	81.7	0.30	0.8	99	-196

Although a seasonal change of H is also observed, it is characterized by smaller amplitude. Monthly mean values of Bowen ratio (ß) are rather low (around 0.3), showing no significant seasonal variation (Table 1). However, the sequence of rainy and sunny periods caused short-term variations of ß between 0.2 and 0.6 with a timescale of about 2 weeks.

Atmos. Chem. Phys. Discuss., doi:10.5194/acp-2017-43, 2017
Manuscript under review for journal Atmos. Chem. Phys.
Discussion started: 10 February 2017

Atmospheric Chemistry and Physics Discussions

Turbulent heat fluxes (H and LE) show a diurnal variation typical of land ecosystems, being in phase with R_n (Fig. 6). The dominance of LE (with respect to H) for northern wetlands has been already reported. Using a flux tower in a Western Siberia bog site located close to Plotnikovo (56˚51' N, 82˚50' E), Shimoyama et al. (2003) show values of ß ranging from 0.57 in the early growing season to 0.78 in the peak growing season. Similar values were found by Aurela et al. (2015) in a Finnish wetland (ß = 0.78, Lompolojänkkä) and in the wetland site Degerö in Sweden (ß = 0.83, Peichl et al. (2013)). However, lower values of ß, more similar to the one in our study, were observed in other northern wetlands (Runkle et al., 2014;Wu et al., 2010;Eugster et al., 2000). Most probably, the difference can be explained by difference in water table depths. One has to account also for the unusually wet conditions in 2015 when the measurements were made, which must have enhanced LE to a certain extent.

The energy balance closure (EBC) for the whole period is around 90% (Fig. 7), meaning that the available energy (R_n-G) is almost equal to the sum of turbulent heat fluxes (H+LE). Monthly estimates of the *EBC* and residual (*Res*) are reported in Table 1. The *EBC* ranges from 87% in May, when the difference between available energy and the turbulent fluxes is 18.8 W m^{-2}, to 129% in August, when *Res* is -20.6 W m^{-2}. The summer months (June and July) show the best values of EBC and Res. The observed values are in line with those from other wetland studies (Kurbatova et al., 2002;Peichl et al., 2013;Runkle et al., 2014). In their FLUXNET site based energy balance closure study, Stoy et al. (2013) reported an average value of 0.76 for the wetland site category, highlighting the relevance of including the heat storage term in sites with high water table depth. Shimoyama et al. (2003) obtained a better EBC value (0.9 vs 0.82 in July), estimating the soil heat flux in the bog from an area averaged value of soil thermal parameter (instead of using a point value), somehow accounting for the surface heterogeneity and the presence of microtopography. The low value of EBC observed in May in Mukhrino probably stems from the high degree of spatial heterogeneity (with part of the ground covered by water), producing high uncertainty in the estimated G. On the other hand, the highest residual found in August (-20.6 W m^{-2}) is mainly due to low data coverage for this month.

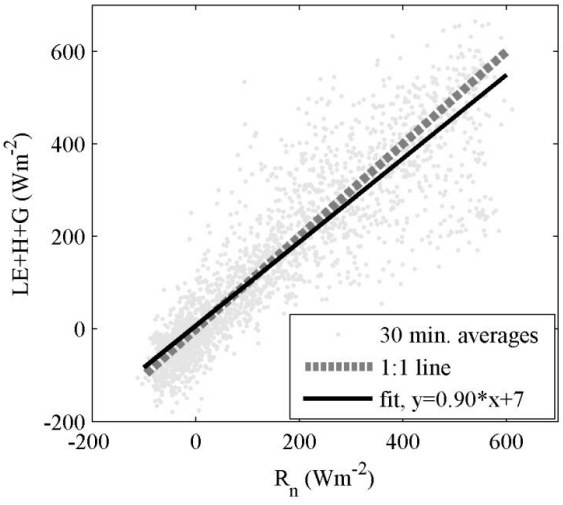

Figure 7: Energy balance plot. The sum of latent and sensible heat fluxes and soil heat flux is plotted against net radiation flux. A linear function is fit to the data and shown together with a 1:1 line.

4.3 Net Ecosystem Exchange

Atmos. Chem. Phys. Discuss., doi:10.5194/acp-2017-43, 2017
Manuscript under review for journal Atmos. Chem. Phys.
Discussion started: 10 February 2017

Atmospheric Chemistry and Physics Discussions

The time-series of measured NEE is shown in Fig. 8a. The largest flux amplitudes are reported during June and July when half-hour values range between -13 μmol m^{-2} s^{-1} and 7 μmol m^{-2} s^{-1}. In May, the measured NEE has a narrower amplitude because of lower temperature and PAR values. Monthly differences in the NEE amplitude can be clearly seen in Fig. 9, where the mean diurnal course is plotted for each month. The modelled NEE, calculated as (R_e-GPP), follows very closely the measured NEE in each month, except in August when R_e is underestimated. As expected, the largest carbon uptake was observed in June and July (-68 and -78 gC m^{-2}, respectively), while in May the cumulative sum of NEE was -35 gC m^{-2}. Unfortunately, poor data coverage was achieved in August, making the corresponding monthly cumulative value somewhat more uncertain, although it seems to have been rather low (-15 gC m^{-2}). Overall, the bog site acted as a net CO_2 sink in the analyzed period. The cumulative gap-filled NEE for of May-August was -196 gC m^{-2}, which decomposes into 162 gC m^{-2} of R_e and -358 gC m^{-2} of GPP. For the period of May-July having the best data coverage, the corresponding values were -181, 127 and -308 gC m^{-2}. Compared with other wetland studies, the net summer uptake observed in Mukhrino was among the highest estimates. For example, Friborg et al. (2003) reported an averaged CO_2 uptake of -7545 mg m^{-2} d^{-1} (which corresponds to a cumulative sum of -64 g C m^{-2}) measured in July by EC system located at the Bakchar bog close to Plotnikovo village in West Siberia. This value is very close to the Mukhrino NEE sum of July alone (Table 1). Lower CO_2 uptake is reported for Zotino bog, where growing season (May-October) cumulative NEEs range between -43 and -60 g C m^{-2} in different years, with maximum daily mean NEE of about -2 μmol m^{-2} s^{-1} measured in July 2000 (Arneth et al., 2002). A similar NEE range of -50 to -90 gC m^{-2} $year^{-1}$ was shown by several peatlands of Northern European Russia and Siberia (Dolman et al., 2012). Daily net carbon uptakes ranging between -1 and -2.8 g C m^{-2} d^{-1} were measured during summer in other northern peatlands in Canada (Humphreys et al., 2006).

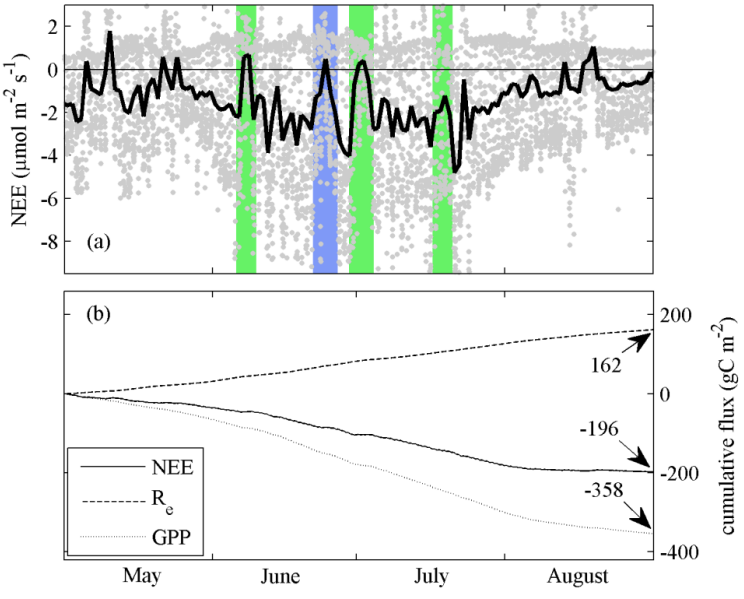

Figure 8: (a) Seasonal variation of NEE measured with the eddy-covariance system; the grey dots correspond to 30 min averages and the black line to the daily averages. The rainy fronts are marked with green and the rain-free front with blue. (b) Cumulative NEE, R_e and GPP.

Atmos. Chem. Phys. Discuss., doi:10.5194/acp-2017-43, 2017
Manuscript under review for journal Atmos. Chem. Phys.
Discussion started: 10 February 2017

Atmospheric Chemistry and Physics Discussions

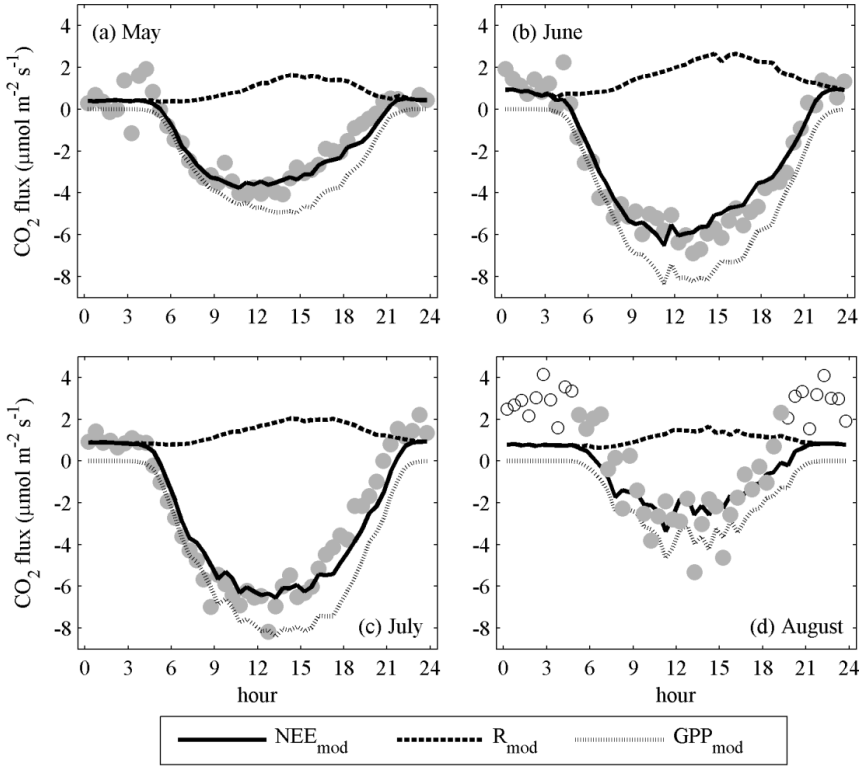

Figure 9: Mean diurnal course of NEE and its components for individual months during the study period. The time in the x-axis corresponds to local winter time (UTC+5). Open circles indicate the nocturnal August data excluded from analysis.

4.4 The effect of weather conditions

The year 2015 was wet and cool in West Siberia. Carbon uptake became significantly limited during the passage of four cold fronts that occurred in June and July (see Fig. 8), three of which were associated with ample precipitation. Uptake plunged to very low values, with the ecosystem even becoming a net CO_2 source during the first three rainy periods. Excluding the rain-free front in late June, each event brought about 100 mm of precipitation, causing WT raises of 8-11 cm (Fig. 4 d,e). However, no dependency of surface exchange on WT was found. The regular and ample precipitation helped sustain water level at a nearly constant level, which was about -60 cm in ridges. In a landscape dominated by ridges (in terms of green biomass), drawdown in WT leads to its decoupling from the hydrological state of surface peat (Price et al., 2003), and, therefore, all vegetation functions including photosynthesis. Sustaining high water level must prevent water stress in the hummock vegetation, which constitutes a significant fraction of green biomass in Mukhrino. In such exceptionally wet conditions as in 2015, the top peat must have stayed moisturized most of the time, meaning that water availability was not the limiting factor for CO_2 uptake. At the same time, the hollows stayed largely inundated and as such probably made a smaller contribution to photosynthesis than hummocks.

The overcast conditions during front passage also resulted in temperature drops by up to 13 degrees. This obviously limited respiration, but also restricted photosynthesis as the optimum growth temperature seems to be close to 30 ˚C

Atmos. Chem. Phys. Discuss., doi:10.5194/acp-2017-43, 2017
Manuscript under review for journal Atmos. Chem. Phys.
Discussion started: 10 February 2017

(Fig. 10). In contrast, between the fronts, air temperatures did occasionally exceed 25 ˚C periodically, promoting photosynthesis. This behavior reflects the temperature control on GPP that is common for the whole Boreal region (Reichstein et al., 2007).

High relative humidity, and thus lower VPD, must have partly compensated for the lower CO_2 uptake during the fronts by promoting higher stomatal conductance (g_s). In terms of the parameters g_1 and m (Fig. 11), the response of g_s to VPD was similar to that in southern Swedish bog Fäjemyr, northern Swedish fen Degerö and southern Finnish fen Siikaneva (Alekseychik et al., unpublished data, Peichl et al., 2013). Mean bulk surface resistance (r_s, the reciprocal of conductance) of 74 s m^{-1} is somewhat lower than approximately 85 s m^{-1} reported for the "wetlands" ecosystem class by (Kasurinen et al., 2014). As mentioned above, the Bowen ratio was stable throughout the summer (~0.3), but the weekly mean values varied between 0.2 and 0.6 in close correlation with the precipitation and cloudiness pattern.

No flux variation with wind direction was found in consistency with the high homogeneity of the landscape within the EC footprint (Fig. 1c-d).

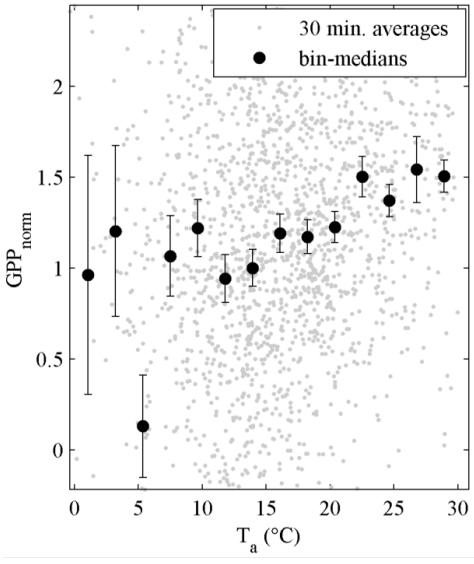

Figure 10: GPP normalized by its model *versus* air temperature. The grey dots are the 30-min average data, and the black circles with error bars the bin-medians. GPP_{norm} saturates approaching 25 ˚C.

Atmos. Chem. Phys. Discuss., doi:10.5194/acp-2017-43, 2017
Manuscript under review for journal Atmos. Chem. Phys.
Discussion started: 10 February 2017

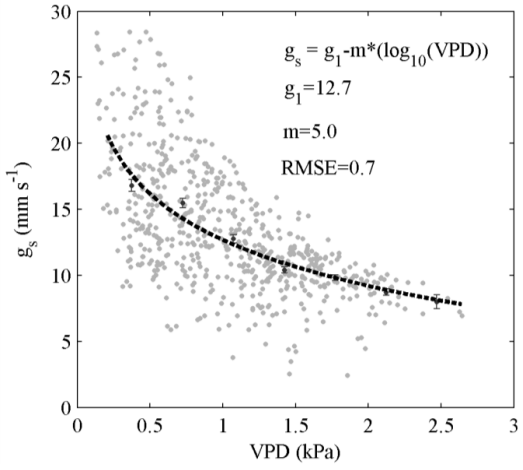

Figure 11: Surface conductance *versus* vapor pressure deficit demonstrating a well-known relationship. The grey dots are the 30-min average data, black dots with error bars the bin-averages, and the dashed line the fit (the function is specified in the insert).

5. Conclusions

This study provides the results of direct and continuous measurements of surface energy balance components and CO_2 flux at the Mukhrino bog site in West Siberian middle taiga. The turbulent fluxes measured by the EC technique over May-August 2015 represent the pioneering dataset of its kind for the region.

The observed magnitudes and diurnal course of sensible and latent heat fluxes were generally in agreement with previous bog studies. The latent heat flux was about three times larger than the sensible heat, and the monthly mean Bowen ratio did not show any significant seasonal variation. However, short-term variations related to heavy rainfall events were observed. In terms of monthly averages, May and June were characterized with the highest available energy.

Carbon dioxide exchange was typical of a raised bog, with net CO_2 sink being rather high (196 gC m^{-2} for May-August) but within the range of previous observations (IPCC, 2014, 2013). Remarkably wet weather of 2015 ensured high moisture availability and thus promoted high photosynthesis during the sunny periods. However, the rainy and cool conditions during the passage of several fronts limited photosynthesis so that the ecosystem temporarily turned into net CO_2 source. The peak in carbon uptake lagged the maximum available energy by one month, falling on June-July. It was apparently modulated by the course of vascular plant leaf area development, which was not measured during the study period.

The Mukhrino station was established for the purpose of long term monitoring of ecosystem functioning and greenhouse gas exchange and continued its operation in 2016. Obtaining a measurement record over several years with varying weather would be instrumental for determining the typical budgets of the ecosystem, unaffected by untypical weather, which was the case in 2015.

Author contributions

P. Alekseychik analyzed the data, produced the figures and contributed to the text. I. Mammarella wrote a major part of the text. D. Karpov and S. Dengel set up the eddy-covariance measurements, provided technical support and contributed to the text. I. Terentieva, A. Sabrekov and M. Glagolev participated in the writing process. E. Lapshina supervised the Mukhrino field station.

Acknowledgements

The study was supported by INTERACT project GHG-FLUX, EU-project GHG-LAKE (project no. 612642), Nordic Centre of Excellence DEFROST, National Centre of Excellence (272041), ICOS-FINLAND (281255) and CarLAC (281196), funded by the Academy of Finland, and the Russian Foundation for Basic Research grant №15-05-07622. The help in the field and provision of data by Yaroslav Solomin and Prof. Martin Heimann is gratefully acknowledged. Nina Filippova compiled the meteorological data. The codes and data used in this study are available upon request.

References

Alekseychik, P., Lappalainen, H., Petäjä, T., Zaitseva, N., Heimann, M., Laurila, T., Lihavainen, H., Eija, E., Arshinov, M., Shevchenko, V., Makshtas, A., Dubtsov, S., Mikhailov, E., Lapshina, E., Kirpotin, S., Kurbatova, Y., Ding, A., Guo, H., Park, S., Lavric, J., Reum, F., Panov, A., Prokushkin, A., and Kulmala, M.: Ground-based station network in arctic and subarctic eurasia: an overview, Geogr. Environ. Sustain., 9, 75-88, 10.15356/2071-9388_02v09_2016_06, 2016.

Arneth, A., Kurbatova, J., Kolle, O., Shibistova, O. B., Lloyd, J., Vygodskaya, N. N., and Schulze, E.-D.: Comparative ecosystem–atmosphere exchange of energy and mass in a European Russian and a central Siberian bog II. Interseasonal and interannual variability of CO2 fluxes, 54, 10.3402/tellusb.v54i5.16684, 2002.

Aurela, M.: The timing of snow melt controls the annual CO2 balance in a subarctic fen, Geophys. Res. Lett., 31, 10.1029/2004gl020315, 2004.

Aurela, M., Lohila, A., Tuovinen, J.-P., Hatakka, J., Penttila, T., and Laurila, T.: Carbon dioxide and energy flux measurements in four northern-boreal ecosystems at Pallas, Boreal Environ. Res., 20, 455-473, 2015.

Belova, S.E., Oshkin, I.Yu., Glagolev, M.V., Lapshina, E.D., Maksyutov, Sh.Sh., Dedysh, S.N.: Methanotrophic Bacteria in Cold Seeps of the Floodplains of Northern Rivers, Microbiology, 82, 743-750, 2013.

Bleuten, W., and Filippov, I.: Hydrology of mire ecosystems in central West Siberia: the Mukhrino Field Station, Transactions of UNESCO department of Yugorsky State University “Dynamics of environment and global climate change”/Glagolev MV, Lapshina ED (eds.). Novosibirsk: NSU, 208-224, 2008.

Bubier, J. L., Bhatia, G., Moore, T. R., Roulet, N. T., and Lafleur, P. M.: Spatial and temporal variability in growing-season net ecosystem carbon dioxide exchange at a large peatland in Ontario, Canada, Ecosystems, 6, 353-367, 2003.

Bulatov, V. I. E.: Geography and ecology of Khanty-Mansiysk and its natural surroundings (In Russian) (География и экология города Ханты-Мансийска и его природного окружения), "Informatsionno-Izdatel’skiy Tsentr", Khanty-Mansiysk, Russia, 187 pp., 2007.

Dolman, A. J., Shvidenko, A., Schepaschenko, D., Ciais, P., Tchebakova, N., Chen, T., van der Molen, M. K., Belelli Marchesini, L., Maximov, T. C., Maksyutov, S., and Schulze, E. D.: An estimate of the terrestrial carbon budget of Russia using inventory-based, eddy covariance and inversion methods, Biogeosciences, 9, 5323-5340, 10.5194/bg-9-5323-2012, 2012.

Eugster, W., Rouse, W. R., Pielke Sr, R. A., McFadden, J. P., Baldocchi, D. D., Kittel, T. G. F., Chapin, F. S., Liston, G. E., Vidale, P. L., Vaganov, E., and Chambers, S.: Land–atmosphere energy exchange in Arctic tundra and boreal forest: available data and feedbacks to climate, Glob. Change Biol., 6, 84-115, 10.1046/j.1365-2486.2000.06015.x, 2000.

Filippova, N. V., Bulyonkova, T. M., and Lapshina, E. D.: Fleshy fungi forays in the vicinities of the YSU Mukhrino field station (Western Siberia), Environ. Dyn. Glob. Clim. Change, 6, 2015.

Friborg, T., Soegaard, H., Christensen, T. R., Lloyd, C. R., and Panikov, N. S.: Siberian wetlands: Where a sink is a source, Geo. Res. Lett., 30, 10.1029/2003GL017797, 2003.

Glagolev, M., Kleptsova, I., Filippov, I., Maksyutov, S., and Machida, T.: Regional methane emission from West Siberia mire landscapes, Environ. Res. Lett., 6, 045214, 10.1088/1748-9326/6/4/045214, 2011.

Golovatskaya, E. A., and Dyukarev, E. A.: Carbon budget of oligotrophic mire sites in the Southern Taiga of Western Siberia, Plant and Soil, 315, 19-34, 10.1007/s11104-008-9842-7, 2008.

Granberg, G., Grip, H., Löfvenius, M. O., Sundh, I., Svensson, B. H., and Nilsson, M.: A simple model for simulation of water content, soil frost, and soil temperatures in boreal mixed mires, Water Resour. Res., 35, 3771-3782, 10.1029/1999WR900216, 1999.

Humphreys, E. R., Lafleur, P. M., Flanagan, L. B., Hedstrom, N., Syed, K. H., Glenn, A. J., and Granger, R.: Summer carbon dioxide and water vapor fluxes across a range of northern peatlands, J. Geophys. Res.: Biogeosciences, 111, 10.1029/2005JG000111, 2006.

IPCC: Supplement to the 2006 IPCC Guidelines for National Greenhouse Gas Inventories: Wetlands, in, edited by: Hiraishi, T., Krug, T., Tanabe, K., Srivastava, N., Baasansuren, J., Fukuda, M., and Troxler, T. G., IPCC, Switzerland, 2014, 2013.

Kasurinen, V., Alfredsen, K., Kolari, P., Mammarella, I., Alekseychik, P., Rinne, J., Vesala, T., Bernier, P., Boike, J., Langer, M., Marchesini, L. B., Van Huissteden, K., Dolman, H., Sachs, T., Ohta, T., Varlagin, A., Rocha, A., Arain, A., Oechel, W., Lund, M., Grelle, A., Lindroth, A., Black, A., Aurela, M., Laurila, T., Lohila, A., and Berninger, F.: Latent heat exchange in the boreal and arctic biomes, Glob. Change Biol., 20, 3439-3456, 10.1111/gcb.12640, 2014.

Kormann, R., and Meixner, F. X.: Boundary-Layer Meteorology, 99, 207-224, 10.1023/a:1018991015119, 2001.

Kurbatova, J., Arneth, A., Vygodskaya, N. N., Kolle, O., Varlargin, A. V., Milyukova, I. M., Tchebakova, N. M., Schulze, E. D., and Lloyd, J.: Comparative ecosystem–atmosphere exchange of energy and mass in a European Russian and a central Siberian bog I. Interseasonal and interannual variability of energy and latent heat fluxes during the snowfree period, Tellus B, 54, 10.3402/tellusb.v54i5.16683, 2002.

Lafleur, P. M., Roulet, N. T., Bubier, J. L., Frolking, S., and Moore, T. R.: Interannual variability in the peatland-atmosphere carbon dioxide exchange at an ombrotrophic bog, Global Biogeochemical Cy., 17, 103610.1029/2002gb001983, 2003.

Mammarella, I., Launiainen, S., Gronholm, T., Keronen, P., Pumpanen, J., Rannik, U., and Vesala, T.: Relative Humidity Effect on the High-Frequency Attenuation of Water Vapor Flux Measured by a Closed-Path Eddy Covariance System, J. Atmos. Ocean. Tech., 26, 1856-1866, 10.1175/2009JTECHA1179.1, 2009.

Mammarella, I., Peltola, O., Nordbo, A., Järvi, L., and Rannik, Ü.: Quantifying the uncertainty of eddy covariance fluxes due to the use of different software packages and combinations of processing steps in two contrasting ecosystems, Atmos. Meas. Tech., 9, 4915-4933, 10.5194/amt-9-4915-2016, 2016.

Masing, V., Botch, M., and Läänelaid, A.: Mires of the former Soviet Union, Wetlands Ecol. Manage., 18, 397-433, 2010.

Ochsener, T., Sauer, T., and Horton, R.: Soil heat storage measurements in energy balance studies, Agron. J., 99, 311-319, 2007.

Oshkin, I. Y., Wegner, C. E., Luke, C., Glagolev, M. V., Filippov, I. V., Pimenov, N. V., Liesack, W., and Dedysh, S. N.: Gammaproteobacterial methanotrophs dominate cold methane seeps in floodplains of West Siberian rivers, Appl. Environ. Microbiol., 80, 5944-5954, 10.1128/AEM.01539-14, 2014.

Peichl, M., Sagerfors, J., Lindroth, A., Buffam, I., Grelle, A., Klemedtsson, L., Laudon, H., and Nilsson, M. B.: Energy exchange and water budget partitioning in a boreal minerogenic mire, J. Geophys. Res.: Biogeosciences, 118, 1-13, 10.1029/2012JG002073, 2013.

Price, J. S., Heathwaite, A. L., and Baird, A. J.: Hydrological processes in abandoned and restored peatlands: An overview of management approaches, Wetlands Ecol. and Manage., 11, 65-83, 10.1023/a:1022046409485, 2003.

Reichstein, M., Papale, D., Valentini, R., Aubinet, M., Bernhofer, C., Knohl, A., Laurila, T., Lindroth, A., Moors, E., Pilegaard, K., and Seufert, G.: Determinants of terrestrial ecosystem carbon balance inferred from European eddy covariance flux sites, Geophys. Res. Lett., 34, L01402, 10.1029/2006gl027880, 2007.

Runkle, B. R. K., Wille, C., Gažovič, M., Wilmking, M., and Kutzbach, L.: The surface energy balance and its drivers in a boreal peatland fen of northwestern Russia, J. Hydrol., 511, 359-373, http://dx.doi.org/10.1016/j.jhydrol.2014.01.056, 2014.

Sabrekov, A., Kleptsova, I., Glagolev, M., Maksyutov, S. S., and Machida, T.: Methane emission from middle taiga oligotrophic hollows of Western Siberia, Tomsk State Pedagogical University Bulletin, 107, 2011.

Sabrekov, A. F., Glagolev, M. V., Kleptsova, I. E., Machida, T., and Maksyutov, S. S.: Methane emission from mires of the West Siberian taiga, Eurasian Soil Sci., 46, 1182-1193, 10.1134/s1064229314010098, 2013.

Schneider, J., Kutzbach, L., and Wilmking, M.: Carbon dioxide exchange fluxes of a boreal peatland over a complete growing season, Komi Republic, NW Russia, Biogeochemistry, 111, 485-513, 10.1007/s10533-011-9684-x, 2011.

Shimoyama, K., Hiyama, T., Fukushima, Y., and Inoue, G.: Seasonal and interannual variation in water vapor and heat fluxes in a West Siberian continental bog, J. Geophys. Res.-Atmospheres, 108, 4648, 10.1029/2003jd003485, 2003.

Shulze, E.-D., Lapshina, E., Filippov, I., Kuhlmann, I., and Mollicone, D.: Carbon dynamics in boreal peatlands of the Yenisey region, western Siberia, Biogeosciences, 12, 7057-7070, 2015.

Stepanova, V. A., and Pokrovsky, O. S.: Macroelement composition of raised bogs peat in the middle taiga of Western Siberia (the bog complex Mukhrino) (In Russian) (Макроэлементный состав торфа выпуклых верховых болот средней тайги Западной Сибири (на примере болотного комплекса «Мухрино»)), Tomsk State University Journal, 352, 211-214, 2011.

Stoy, P. C., Mauder, M., Foken, T., Marcolla, B., Boegh, E., Ibrom, A., Arain, M. A., Arneth, A., Aurela, M., Bernhofer, C., Cescatti, A., Dellwik, E., Duce, P., Gianelle, D., van Gorsel, E., Kiely, G., Knohl, A., Margolis, H., McCaughey, H., Merbold, L., Montagnani, L., Papale, D., Reichstein, M., Saunders, M., Serrano-Ortiz, P., Sottocornola, M., Spano, D., Vaccari, F., and Varlagin, A.: A data-driven analysis of energy balance closure across FLUXNET research sites: The role of landscape scale heterogeneity, Agr. Forest Meteorol., 171–172, 137-152, http://dx.doi.org/10.1016/j.agrformet.2012.11.004, 2013.

Szajdak, L. W., Lapshina, E. D., Gaca, W., Styla, K., Meysner, T., Szczepanski, M., and Zarov, E. A.: Physical, chemical and biochemical properties of Western Siberia Sphagnum and Carex peat soils, Environ. Dyn. Glob. Clim. Change, 7, 13-25, 2016.

Terentieva, I., Glagolev, M., Lapshina, E., Sabrekov, A., and Maksyutov, S.: High resolution wetland mapping in West Siberian taiga zone for methane emission inventory, Biogeosciences, 13, 4615–4626, 2015.

Turunen, J., Tahvanainen, T., Tolonen, K., and Pitkänen, A.: Carbon accumulation in West Siberian mires, Russia Sphagnum peatland distribution in North America and Eurasia during the past 21,000 years, Glob. Biogeochemical Cy., 15, 285-296, 2001.

van Dijk, A., Moene, A. F., and de Bruin, A. R.: The principles of surface flux physics: Theory, practice and description of the ECPack library., Meteorology and Air Quality Group, Wageningen University, Wageningen, The Netherlands, 99, 2004.

Webb, E. K., Pearman, G. I., and Leuning, R.: Correction of Flux Measurements for Density Effects due to Heat and Water-Vapor Transfer, Q. J. Roy. Meteor. Soc., 106, 85-100, 1980.

Weiss, R., Alm, J., Laiho, R., and Laine, J.: Modeling moisture retention in peat soils, Soil Sci. Soc. Am. J., 62, 305-313, 1998.

Vickers, D., and Mahrt, L.: Quality Control and Flux Sampling Problems for Tower and Aircraft Data, J. Atmos. Ocean. Tech., 14, 512-526, 10.1175/1520-0426(1997)014<0512:qcafsp>2.0.co;2, 1997.

Wu, J., Kutzbach, L., Jager, D., Wille, C., and Wilmking, M.: Evapotranspiration dynamics in a boreal peatland and its impact on the water and energy balance, J. Geophys. Res.: Biogeosciences, 115, 10.1029/2009JG001075, 2010.

Yu, Z. C.: Northern peatland carbon stocks and dynamics: a review, Biogeosciences, 9, 4071-4085, 10.5194/bg-9-4071-2012, 2012.

Yurova, A., Wolf, A., Sagerfors, J., and Nilsson, M.: Variations in net ecosystem exchange of carbon dioxide in a boreal mire: Modeling mechanisms linked to water table position, J. Geophys. Res.: Biogeosciences, 112, 10.1029/2006JG000342, 2007.